

S.R. GORELIK[✉]
E.N. CHESNOKOV
A.V. KUIBIDA
R.R. AKBERDIN
A.K. PETROV

Infrared multiphoton dissociation of difluorosilane

Institute of Chemical Kinetics and Combustion of SB RAS, Institutskaya, 3, Novosibirsk 630090, Russia

Received: 27 March 2003/Revised version: 5 August 2003
Published online: 18 November 2003 • © Springer-Verlag 2003

ABSTRACT Infrared (IR) multiphoton absorption and dissociation of difluorosilane molecules under the action of a pulsed transversely excited atmospheric CO₂ laser were experimentally studied. It has been found that the multiphoton absorption is strongly saturated due to the rotational bottleneck effect. Isotope-selective IR multiphoton dissociation of difluorosilane was performed at 977.2 cm⁻¹. The dissociation rate for ²⁸SiH₂F₂ isotopomer has been found to be about twice as high as for the other isotopomers at this wavelength.

PACS 82.50.Bc; 82.30.Lp

1 Introduction

In the past few years the interest in isotopically pure silicon materials has been growing in the world. It arises from prospects of application of these materials for semiconductor technology. For example, it was shown that the thermal conductivity and the electric conductivity in ²⁸Si isotopically pure monocrystals are much higher compared to those with natural isotope composition [1, 2]. This fact might be required in particular for creating more powerful computer processors even today.

Silicon has three stable isotopes with the natural composition: 92.22% (²⁸Si) : 4.69% (²⁹Si) : 3.09% (³⁰Si) [9]. Separation of Si isotopes by means of infrared laser radiation had been studied in [3–8]. Except for the earliest demonstrations in which the isotope-selective infrared multiphoton dissociation (IR MPD) of SiF₄ [3] and the isotope-selective reaction of bromination of vibrationally excited silane [4] were studied, all the other works studied IR MPD of the species Si₂F₆ [5–9]. Kamioka et al. [5, 6] reported the IR MPD of Si₂F₆ molecules induced by CO₂-laser radiation with high dissociation efficiency and high isotope selectivity. High dissociation yield had been reached with mild radiation fluences lower than 1 J/cm². The dissociation products were stable molecules (SiF₄) and low-active radicals (SiF₂). The isotope composition of the SiF₄ product varied depending on the wavelength of the CO₂-laser radiation. The maximum isotope content of

³⁰Si in SiF₄ was nearly 50%, and for ²⁹Si it was about 12%. It was demonstrated in these works that the isotope-selective IR MPD of the Si₂F₆ molecules can be the basis for the technological process of silicon-isotope separation with productivity of several grams per hour of the dissociation products enriched by 33% of ³⁰Si.

Despite such impressive results, it is not evident that Si₂F₆ might be considered as the best object for silicon-isotope separation by IR MPD. The molecule contains two Si atoms and the rear isotopes are contained mostly in 'isotopically mixed' molecules such as F₃²⁸Si–²⁹SiF₃ and F₃²⁸Si–³⁰SiF₃. This fact limits the isotopic effect since during the dissociation of such 'isotopically mixed' molecules, the ²⁸Si isotope and the rear one, (²⁹Si or ³⁰Si), would pass into products equally. Let us note that, in the experiments reported in [5, 6], this limit for the ³⁰Si-isotope enrichment was reached. Besides, the isotopic shift of the molecular vibrational frequencies in the 'isotopically mixed' molecules should be less than that in the 'isotopically pure' molecules.

The above arguments set the problem of searching for molecules containing only one silicon atom and which are at least as effective for isotope-selective IR MPD as Si₂F₆. To solve this problem, the systematic quantitative experimental investigation of the IR multiphoton absorption (IR MPA) and IR MPD of molecules with only one silicon atom is necessary.

The present paper describes the experimental investigation of the main features of the IR MPA and IR MPD of the species SiH₂F₂ under the action of a CO₂ laser.

2 Experiment

As a source of IR radiation, a home-made pulsed transversely excited atmospheric CO₂ laser was used. The maximum laser output energy was about 1 J per pulse and the maximum pulse-repetition rate was 1 Hz. The laser-beam cross section was about 1 × 2.5 cm² and the divergence was about 0.5 × 10⁻³ rad. Almost all experimental data have been obtained with a uniform laser beam. Two confocal lenses with focal lengths of 58 cm and 29 cm were used to increase the laser-radiation energy fluence. To decrease the fluence significantly, a set of parallel-sided CaF₂ plates was used. For smooth variation of the fluence, a silicon parallel-sided plate was used. The plate transmission could vary from about 100%, when the incident angle was about 76°, down to 60%

✉ Fax: +7-3832/342-350, E-mail: gorelik@rs.noda.sut.ac.jp

at the normal incidence of the laser beam. The laser beam was collimated at the input of the reaction cell by an orifice of 4.5-mm diameter.

All the experiments were performed in batch-cell conditions. The reaction cell was a Pyrex-glass cylinder with NaCl windows. The cell length was 18 cm with a diameter of 3 cm. The cell had a finger to freeze the cell's contents in liquid nitrogen and a thermocouple vacuum gauge to measure the pressure of non-freezing components of the cell contents.

In front of the input cell window and behind the output one, two NaCl beam splitters were placed at 45° to the laser beam. They reflected a small part of the laser beam into two pyroelectric detectors. To eliminate errors due to the laser-beam spatial non-uniformity, scatter filters were placed in front of each pyroelectric detector. The output signals from the detectors were transferred through an analog to digital converter into the PC. Their ratio was used for measuring low absorption of the laser radiation in the cell. The experimental conditions were chosen to cause the absorption in the cell not to exceed 10%.

The absolute value of the average laser-pulse energy was controlled by an optical power meter.

The initial sample pressure was controlled by a diaphragm pressure gauge and was varied within 0.5–1 Torr throughout all experiments.

The SiF_2H_2 reduction due to dissociation was controlled by IR spectra. A Fourier-transform infrared (FTIR) spectrometer (Bruker Vector 22) was used. The total quantitative analysis of gas-phase dissociation products was performed with a mass spectrometer. The products were SiF_4 , H_2 and SiF_3H . From all the products, only the hydrogen was non-freezing at the liquid-nitrogen temperature. This fact can be used as a basis for a quite sensitive and relatively simple method of measuring the dissociated part of the sample molecules. After the sample was irradiated by a certain number of laser pulses, all the reaction-cell contents except H_2 were frozen in the finger by liquid nitrogen. The H_2 concentration was detected by the thermocouple gauge calibrated for H_2 . In special experiments with the FTIR spectrometer, it was checked that the amount of produced H_2 was equal to the amount of the dissociated sample. The irradiation time was chosen so that the pressure of the produced H_2 would not exceed 100 mTorr.

Difluorosilane was synthesized by the reaction of dichlorosilane with SbF_3 with the reaction yield of about 80% and was used after low-temperature distillation. Distilled SiF_2H_2 contained 4% of SiF_3H as impurity. This impurity appeared to be difficult to eliminate by distillation due to the small difference of vapor pressures of SiF_2H_2 and SiF_3H .

3 Results and discussion

3.1 Multiphoton absorption in SiF_2H_2

SiF_2H_2 molecules have an intensive absorption band in the spectral region of CO_2 -laser radiation corresponding to the Si–F antisymmetric stretch vibration $\nu_8 = 981.7 \mu\text{m}^{-1}$ [10]. The IR spectrum of this band measured by the FTIR spectrometer with 1-cm^{-1} resolution is shown in Fig. 1. The absorption cross section was calculated from the measured absorbance, the reaction-cell length and the concen-

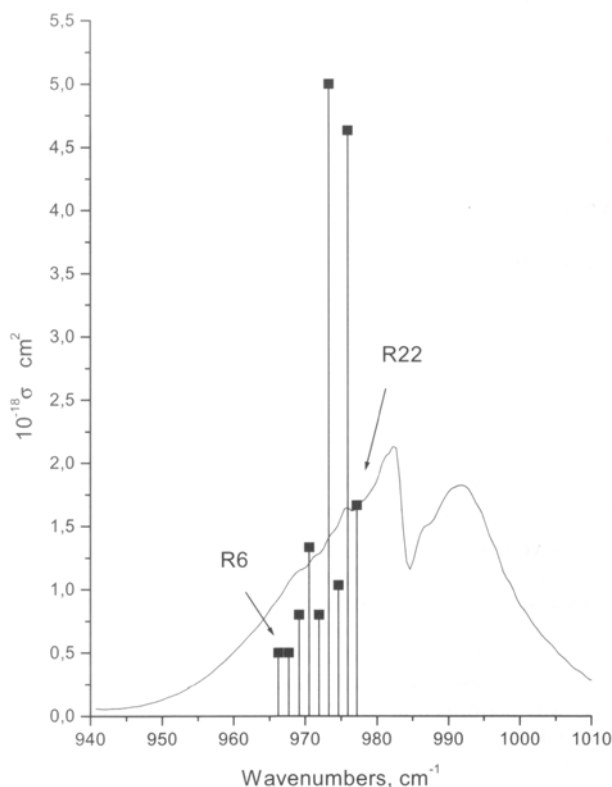


FIGURE 1 Linear absorption spectrum of difluorosilane, 1 Torr, in spectral region of Si–F stretching vibrations. Solid line – absorption cross section, measured by FTIR spectrometer with 1-cm^{-1} resolution, squares with vertical lines – measurements of continuous-wave CO_2 -laser radiation absorption

tration of SiF_2H_2 molecules. The rotational structure of the spectrum was not observed at such resolution. The spectral width of the CO_2 -laser radiation is less than 0.2 cm^{-1} . Therefore, the absorption of the laser radiation could be different from that measured by the FTIR spectrometer. The absorption cross sections measured for different CO_2 -laser lines are shown in Fig. 1 by vertical solid lines. A continuous-wave CO_2 laser was used to avoid saturation of the linear absorption. The obtained values are close to or even lower than those measured by the FTIR spectrometer for almost all laser lines. It was only for 10R(16) and 10R(20) laser lines that the absorption cross sections were 2–3 times higher than those measured by the FTIR spectrometer, showing that the rotational structure was not completely eliminated.

The results of the absorption of the pulsed CO_2 -laser radiation in SiF_2H_2 are shown in Figs. 2 and 3.

The IR MPA spectrum obtained by tuning the pulsed CO_2 laser through the laser lines is shown in Fig. 2. It is smoother than the linear one as obtained by a continuous-wave CO_2 laser and no sharp changes in absorption were observed between any two neighboring lines.

Figure 3 presents the laser-fluence dependence of $\langle n \rangle$ – the average number of absorbed photons per molecule per pulse for the 10R(22) CO_2 laser line. The dependence could be approximated as $\langle n \rangle \sim \Psi^{0.67}$ in a quite wide range of fluence Ψ . It is only at fluences higher than 0.3 J/cm^2 that $\langle n \rangle$ goes lower than could be predicted by this formula.

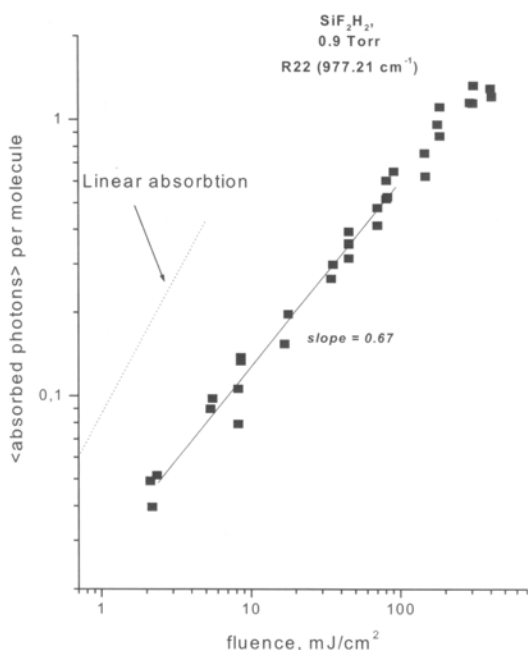


FIGURE 2 CO₂-laser radiation energy fluence dependence of IR MPA at 10R(22) CO₂-laser line (977.2 cm⁻¹). Dashed line – extrapolated linear absorption. Sample pressure – 0.9 Torr

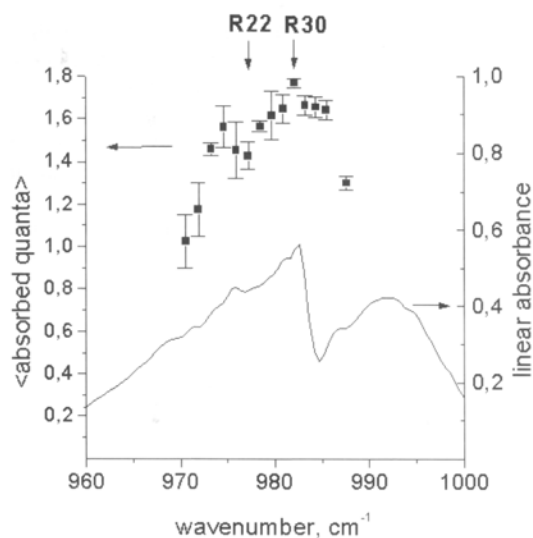


FIGURE 3 SiF₂H₂ IR MPA spectrum at fixed laser fluence of 220 mJ/cm². Solid line – linear absorption spectrum. Sample pressure – 0.9 Torr

The dashed line in this figure corresponds to a linear dependence $\langle n \rangle_{\text{lin}} = \sigma_0 \Psi$, where σ_0 is the cross section of the linear absorption (Fig. 1) at the wavelength of the 10R(22) laser line. The experimental points lie much lower than points of the extrapolated linear absorption. It means that the linear absorption is saturated even at radiation fluences less than 10^{-2} J/cm². If all the molecules are involved in the absorption process, the number of absorbed quanta per molecule, which is necessary to provide the strong saturation, $\langle n \rangle_{\text{sat}}$, should be ≥ 0.5 . In our case, the saturation occurs when the average number of absorbed quanta per molecule, $\langle n \rangle_{\text{exp}}$, does

not exceed 0.05. It unambiguously indicates that only a small part of the sample molecules interacts with the radiation. This part is usually called the q -factor [11]. We can estimate q as: $q \approx \langle n \rangle_{\text{exp}} / \langle n \rangle_{\text{sat}}$. Hence, at minimum radiation fluence in our measurements we obtain $q \leq 0.1$.

These results strongly differ from the results on IR MPA of Si₂F₆ as reported in [12]. In that work it was shown that, for the Si₂F₆ molecule, saturation does not occur until $\langle n \rangle$ becomes higher than at least five quanta per molecule and q to be close to 1 for this molecule.

Thus, the IR MPA of the SiF₂H₂ molecules is much weaker than the IR MPA of the Si₂F₆ molecules in the spectral region of CO₂-laser radiation. The main reason is that the q -factor, the part of the molecules interacting with radiation, is small for SiF₂H₂.

The high efficiency of the IR MPA in Si₂F₆ in [12] is explained partly by participation of two- and three-photon transitions. Besides, as was mentioned in [12], the latter molecule has four low-frequency vibrational modes, which generate many low-lying levels significantly populated at room temperature that contribute to absorption.

Let us note that there exists another important factor. For the efficiency of the IR multiphoton excitation process, of crucial importance are intramolecular anharmonic couplings between different vibrational modes in the region of low-lying vibrational levels [13–15, 36]. The strongest non-linear interactions responsible for the coupling are the third- and fourth-order anharmonic terms:

$$V_{\text{nonl}} = \frac{1}{3!} \sum \alpha_{ijk} q_i q_j q_k + \frac{1}{4!} \sum \beta_{ijkl} q_i q_j q_k q_l,$$

q_i being the normal coordinates and α_{ijk} and β_{ijkl} anharmonic force constants.

The role of anharmonic coupling of vibrational modes essentially increases when the frequencies of the vibrational modes hit the resonance conditions $\nu_i \pm \nu_j \pm \nu_k \approx 0$ (three-frequency resonance) and $\nu_i \pm \nu_j \pm \nu_k \pm \nu_m \approx 0$ (four-frequency resonance). If a molecule has enough resonances, at a certain level of excitation all vibrational modes of the molecule will be coupled by the ‘chain’ of anharmonic resonances [13, 16]. The larger the molecule, the greater the number of vibrational modes, and the higher the possibility that they will be coupled by such a ‘chain’ at low vibrational energy. However, there are examples of relatively small molecules for which almost all vibrational modes are coupled by such a ‘chain’ at relatively low energy of excitation and hence are involved in the process of multiphoton absorption. One of such molecules is CF₃I, for which the q -factor is close to 1 due to effective mode mixing through several three-frequency resonances [13, 14].

All the possible symmetry-allowed three- and four-frequency resonances of the normal modes of the SiF₂H₂ molecule in harmonic approximation and their energy deficits are given in Table 1.

Table 1 shows that, in the SiF₂H₂ molecule, the energy deficits ΔE for all the three-frequency resonances are larger than 200 cm⁻¹. In contrast, the CF₃I molecule has three three-frequency resonances within a mere 11 cm⁻¹ [13, 14, 17].

There are four four-frequency resonances with relatively low ΔE in the SiF₂H₂ molecule, but it is only in $\nu_2 + \nu_2 - \nu_8 -$

Symmetry types	A ₁	A ₂	B ₁	B ₂
Mode frequencies, cm ⁻¹	$\nu_1 = 2245.7$ $\nu_2 = 981.7$ $\nu_3 = 869.6$ $\nu_4 = 322$	$\nu_5 = 730$	$\nu_6 = 2250.5$ $\nu_7 = 730$	$\nu_8 = 981$ $\nu_9 = 903.4$
	Third-order resonances		$(\Delta E < 300 \text{ cm}^{-1})$	
1	$\nu_1 - \nu_2 - \nu_2$		$\Delta E = 282.3 \text{ cm}^{-1}$	
2	$\nu_1 - \nu_8 - \nu_8$		$\Delta E = 283.7 \text{ cm}^{-1}$	
3	$\nu_2 - \nu_3 - \nu_4$		$\Delta E = -209.9 \text{ cm}^{-1}$	
4	$\nu_3 - \nu_4 - \nu_4$		$\Delta E = 225.6 \text{ cm}^{-1}$	
5	$\nu_8 - \nu_4 - \nu_9$		$\Delta E = 244.4 \text{ cm}^{-1}$	
	Fourth-order resonances		$(\Delta E < 40 \text{ cm}^{-1})$	
1	$\nu_2 + \nu_2 - \nu_8 - \nu_8$		$\Delta E = 1.4 \text{ cm}^{-1}$	
2	$\nu_2 + \nu_5 - \nu_7 - \nu_8$		$\Delta E = 0.7 \text{ cm}^{-1}$	
3	$\nu_2 + \nu_7 - \nu_5 - \nu_8$		$\Delta E = 0.7 \text{ cm}^{-1}$	
4	$\nu_6 + \nu_6 - \nu_1 - \nu_1$		$\Delta E = 9.6 \text{ cm}^{-1}$	
5	$\nu_1 - \nu_4 - \nu_8 - \nu_8$		$\Delta E = 38.3 \text{ cm}^{-1}$	
6	$\nu_1 - \nu_4 - \nu_8 - \nu_9$		$\Delta E = 39.3 \text{ cm}^{-1}$	
7	$\nu_2 + \nu_3 - \nu_8 - \nu_9$		$\Delta E = 33.1 \text{ cm}^{-1}$	
8	$\nu_2 + \nu_9 - \nu_3 - \nu_8$		$\Delta E = 34.5 \text{ cm}^{-1}$	
9	$\nu_3 + \nu_5 - \nu_7 - \nu_9$		$\Delta E = 33.8 \text{ cm}^{-1}$	
10	$\nu_3 + \nu_7 - \nu_5 - \nu_9$		$\Delta E = 33.8 \text{ cm}^{-1}$	

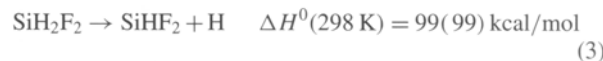
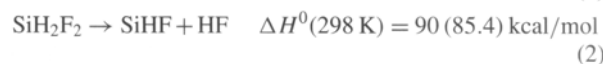
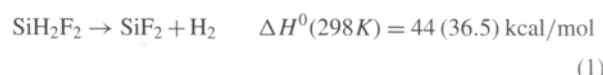
TABLE 1 Normal-mode frequencies of SiH₂F₂ molecule from [10] and possible symmetry-allowed anharmonic resonances of third and fourth orders with their energy deficits ΔE

ν_8 that the pumped mode ν_8 is involved. Other four-frequency resonances require unpumped modes to be initially populated and should not work.

From this point of view, the SiH₂F₂ molecule can be characterized as a ‘unlucky’ system, in which occasionally the number of strong non-linear resonances in the system of low-lying vibrational levels is not enough for effective ‘chain’ mixing of vibrational modes.

3.2 Multiphoton dissociation of SiH₂F₂

A few reaction channels are energetically available for the unimolecular decay of the difluorosilane molecule.



The heats of reactions as calculated using heats of formation for various SiHF compounds were taken from [18]. The quantum chemical calculation [19] gives slightly different values for the heats of reactions (in brackets). The rate constant of the SiH₂F₂ unimolecular decay was measured experimentally as reported in [20]. The measurements were performed at the temperatures of 1190–2150 K, and buffer-gas pressures of 0.25–2 bar, which was within the falloff region. In [20], the weak-collision falloff calculation was reported in which the dissociation energy E_0 was treated as a fitting parameter. Assuming that $\log A_\infty = 13.5 \pm 1$, the value of the threshold $E_0 = 72 \text{ kcal/mol}$ was obtained. Also,

it was about 30 kcal/mol higher than the heat of reaction of channel (1), but it was still lower than the heats of reactions of other channels. Therefore, it was concluded that the most probable pathway for the unimolecular decomposition of SiF₂H₂ was channel (1) with the lowest activation threshold.

SiF₂ is a very low activity radical [21–25]. The rate constant of the reaction of SiF₂H₂ with H₂ at room temperature is lower than $10^{-17} \text{ cm}^3/\text{s}$ [21, 22]. We performed the mass-spectrometric analysis of the reaction-cell contents after 30 min of irradiation. The laser line was 10R(22) and the initial SiF₂H₂ pressure was 0.6 Torr. The laser radiation was focused in the cell center by a 9-cm focal length lens. No disilanes were found in the products, so we assumed that the reaction of SiF₂ with SiF₂H₂ did not take place under our experimental conditions. According to the mass-spectrometric analysis, the main final products were H₂ and SiF₄. It was mentioned in [5, 6] that SiF₂ produced in the IR MPD of Si₂F₆ formed polymers on the walls of the reaction cell. So, we assumed that SiF₄ in our experiments was formed in heterogeneous reactions of SiF₂ with the products of previous experiments on the reaction-cell walls.

The laser radiation energy fluence dependence of the SiF₂H₂ MPD probability is shown in Fig. 4. The laser line was 10R(22) and the experimentally measured value was a pressure of H₂ non-frozen in liquid nitrogen. The MPD probability β becomes measurable at fluences higher than 0.5 J/cm^2 and reaches 3×10^{-3} at about 2 J/cm^2 . We did not increase the radiation fluence higher than 2 J/cm^2 , since it might be dangerous for the input window of the reaction cell. Let us mention for comparison that the MPD probability of Si₂F₆ reached 0.01 at a CO₂-laser energy fluence of about 0.25 J/cm^2 [5].

Figure 5 shows the MPD spectrum of SiF₂H₂ (solid line, top of Fig. 5), obtained by tuning the CO₂-laser radiation over the rotational lines of the laser. The linear absorption spectrum of SiF₂H₂ (0.9 Torr) is shown at the bottom of Fig. 5.

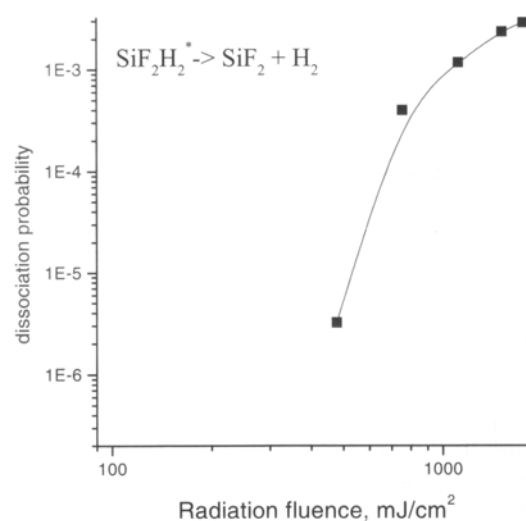


FIGURE 4 Radiation-fluence dependence of IR MPD probability of difluorosilane at the 10R(22) CO₂-laser line (977.2 cm^{-1})

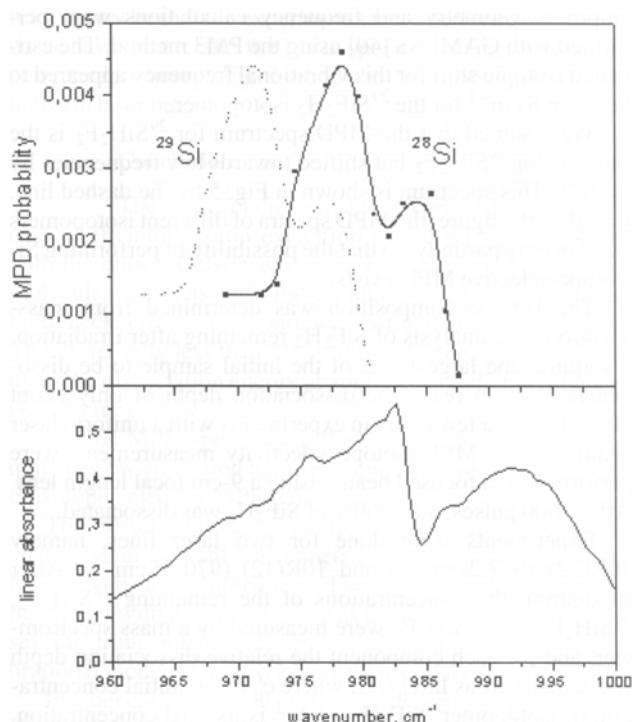


FIGURE 5 Top - experimentally measured SiF₂H₂ IR MPD spectrum at fixed radiation fluence of 1.2 J/cm². Sample pressure - 0.9 Torr. Dotted line - the same spectrum, shifted by 8 cm⁻¹ towards the low-frequency region. Bottom - linear absorption spectrum of 0.9 Torr SiF₂H₂ with natural isotopic abundance; resolution 1 cm⁻¹

3.3 Estimation of q -factor

We can estimate independently the q -factor by comparing SiF₂H₂ MPA and MPD results obtained in the experiments as described above. For this estimation we use the concept of a bimodal energy distribution, formed in the IR multiphoton excitation process.

According to this concept, during the irradiation of molecules with intense IR laser radiation, two molecular ensembles are formed: one, which interacts with radiation - a 'hot' ensemble, and the second, which does not interact with radiation - a 'cold' ensemble [26]. The energy distribution of the molecules can be written as:

$$N(E_v) = (1 - q)F_0(E_v) + qF_1(E_v), \quad (4)$$

where q is the part of the 'hot' molecules and $F_0(E_v)$ and $F_1(E_v)$ are the energy distribution functions for the 'cold' and 'hot' molecular ensembles correspondingly. The distribution function of the 'cold' ensemble is close to the Boltzmann distribution with a vibrational temperature close to room temperature $T_0 = 300$ K [27]. For the 'hot' ensemble, the distribution is not known. For simplicity, we shall assume that the 'hot' ensemble is also characterized by the Boltzmann distribution with a temperature T_1 .

Next, we assume that if the molecule has a vibrational energy higher than the dissociation threshold $E_0 = 72$ kcal/mol, it dissociates. Also, we assume that the mean excitation energy of the molecules in the 'hot ensemble' is significantly lower than the dissociation energy E_0 under our experimental

conditions. So, only the molecules in the 'very tail' of the distribution dissociate, and the dissociation does not significantly perturb the population distribution.

Then, we can express the experimentally measured parameters $\beta(\Psi)$ and $\langle n \rangle(\Psi)$ via the distribution parameters q and T_1 as follows:

$$\beta(\Psi) = qW_{E>E_0}(T_1), \quad (5)$$

$$\langle n \rangle(\Psi) = q\langle n_q(T_1) \rangle, \quad (6)$$

where $W_{E>E_0}(T_1)$ is the probability that at the given temperature the molecule has an energy higher than the dissociation energy, $\langle n_q \rangle$ is the average number of absorbed photons per molecule in the 'hot' ensemble, $\langle n_q \rangle = \langle E_v(T_1) \rangle / h\nu$, $\langle E_v(T_1) \rangle$ is the average vibrational energy of the molecules at the given temperature T_1 and $h\nu$ is the CO₂-laser photon energy.

$W_{E>E_0}(T_1)$ was calculated by numeric integration of the distribution function. The density of vibrational states was calculated using Whitten-Rabinovitch formulae [28] and frequencies of vibrational modes of difluorosilane [10]. The vibrational energy $\langle E_v(T_1) \rangle$ was calculated using the formula for internal energy in harmonic approximation [29]. Calculated dependences of $W_{E>E_0}(T_1)$ and $\langle n_q(T_1) \rangle$ on temperature T_1 are shown in Fig. 6.

Formulae (5) and (6) allow for independent determination of the parameters q and T_1 from the experimentally measured $\beta(\Psi)$ and $\langle n \rangle(\Psi)$. Unfortunately, in our experiments $\beta(\Psi)$ and $\langle n \rangle(\Psi)$ were measured mostly at different Ψ . Only at $\Psi = 0.5$ J/cm² were both parameters measured (Figs. 2 and 4). At this radiation energy fluence we obtain $q = 0.15$ and $T_1 = 1600$ K.

Above we assumed that the molecular distribution in the 'hot' ensemble was of Boltzmann type. The actual molecular energy distribution formed in the process of multiphoton excitation might be different [30-33]. Qualitatively, we could

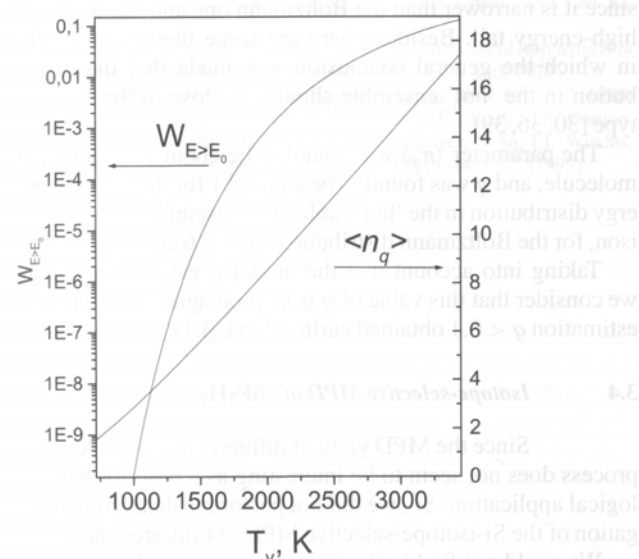


FIGURE 6 Calculated dependences of the part of SiH₂F₂ molecules with energies higher than the dissociation threshold $E_0 = 72$ kcal/mol and average number of vibrational quanta on the vibrational temperature in the 'hot' molecular ensemble with Boltzmann energy distribution

expect that such a 'real' distribution should be narrower and should have a shorter high-energy tail as compared to the Boltzmann distribution for the same mean excitation energy. This conclusion follows from the data available in the literature [14, 30, 34–37]. One of the examples of indirect evidence for a shorter tail is the threshold behavior of the radiation-fluence dependence of the IR MPD yield, typical for almost all studied molecules [30, 36]. In general, since the Boltzmann form of energy distribution corresponds to the maximum entropy distribution of vibrational energy following multiphoton excitation [38, 39], it should be the broadest possible one for any given mean excitation [39].

Let us consider the equation set (5) and (6) for such a 'real' distribution with the fitting parameters q and $\langle n_q \rangle$. Let us mention again that we assume that the average excitation energy is much lower than the dissociation energy E_0 . We can expect the value $W(E > E_0)$ from (6) to be smaller for the 'real' distribution than that for the Boltzmann distribution for the same mean excitation level $\langle n_q \rangle$. Hence, the parameter set q and $\langle n_q \rangle$, which fits the equation set (5) and (6) in the case of the Boltzmann energy distribution, cannot fit it in the case of the 'real' energy distribution. Since the tail of this distribution drops even more sharply than that of the Boltzmann one, we cannot fit the equation set (5) and (6) by decreasing $\langle n_q \rangle$. We can fit this equation set only by increasing $\langle n_q \rangle$. In this case, q should become lower than that calculated for the Boltzmann energy distribution (from (5)). Hence, the estimation of q with the Boltzmann energy distribution gives us the upper limit of q .

To illustrate the above considerations, we have solved the equation set (5) and (6) and have found the parameters q and $\langle n_q \rangle$, assuming the population distribution in the 'hot' ensemble to be of Poisson type $P_n = ((n_q)^n / n!) e^{-n_q}$ [39], where P_n is the probability for finding an energy equivalent to n photons of fixed energy $h\nu$ in the molecules of the 'hot' ensemble, and $\langle n_q \rangle$ represents the mean excitation level in the 'hot' ensemble. We have chosen this distribution function, since it is narrower than the Boltzmann one and has a shorter high-energy tail. Besides, there are some theoretical works in which the general conclusion was made that the distribution in the 'hot' ensemble should be close to the Poisson type [30, 36, 39].

The parameter $\langle n_q \rangle$ was found to be about 10 quanta per molecule, and q was found to be about 0.1 for the Poisson energy distribution in the 'hot' molecular ensemble (by comparison, for the Boltzmann distribution $\langle n_q \rangle \approx 6$ and $q \approx 0.15$).

Taking into account that the model is essentially rough, we consider that this value of q is in good agreement with the estimation $q < 0.1$ obtained earlier (Sect. 3.1).

3.4 Isotope-selective MPD of SiF₂H₂

Since the MPD yield of difluorosilane was low, the process does not seem to be interesting as a base for technological application. So, we did not perform a detailed investigation of the Si-isotope-selective MPD of difluorosilane.

We could not find in the literature any experimental data on the vibrational frequencies of SiF₂H₂ molecules with isotopes ²⁹Si and ³⁰Si. For a rough estimation of the isotopic shift of the Si–F antisymmetric vibrational frequency, semi-

empirical geometry and frequency calculations were performed with GAMESS [40] using the PM3 method. The estimated isotopic shift for this vibrational frequency appeared to be about 8 cm⁻¹ for the ²⁹SiF₂H₂ isotopomer.

We assumed that the MPD spectrum for ²⁹SiH₂F₂ is the same as for ²⁸SiH₂F₂ but shifted towards low frequencies by 8 cm⁻¹. This spectrum is shown in Fig. 5 by the dashed line. Based on the figure, the MPD spectra of different isotopomers overlap only partially, so that the possibility of performing Si-isotope-selective MPD exists.

The isotope composition was determined from mass-spectrometric analysis of SiF₂H₂ remaining after irradiation. It requires the largest part of the initial sample to be dissociated. We can reach the dissociation depth of only about 10%–15% in a few hours in experiments with a uniform laser beam. So, the MPD isotope selectivity measurements were performed in a focused beam, using a 9-cm focal length lens. After 2000 pulses, 30%–60% of SiF₂H₂ was dissociated.

Experiments were done for two laser lines, namely 10R(22) (977.2 cm⁻¹) and 10R(12) (970.55 cm⁻¹). After irradiation, the concentrations of the remaining ²⁸SiH₂F₂, ³⁰SiH₂F₂ and ²⁹SiH₂F₂ were measured by a mass spectrometer, and for each component the relative dissociation depth was calculated as $\ln(c_0^i/c^i)$, where c_0^i is the initial concentration of isotopomer ⁱSiF₂H₂, and c^i is its final concentration. The dependence of the relative dissociation rate on irradiation time for the 10R(22) laser line is shown in Fig. 7. One can see that ²⁸SiH₂F₂ decomposes at this wavelength about two times faster than both ³⁰SiH₂F₂ and ²⁹SiH₂F₂. Let us note that such a ratio of dissociation rates at this wavelength can be predicted from Fig. 5.

In the experiment with the 10R(12) laser line, we did not observe any isotope effect within error limits of 20%. The

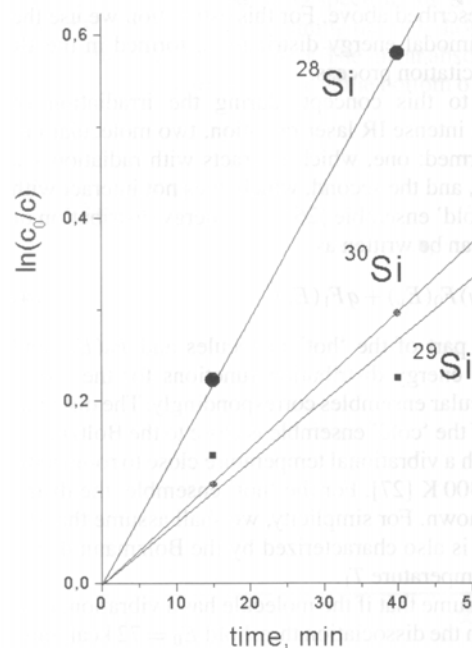


FIGURE 7 Dependence of the MPD rate of SiH₂F₂ molecules, containing different Si isotopes, on irradiation time at the 10R(22) CO₂-laser line (977.2 cm⁻¹) in focused laser beam

reason may be that the experiments were performed in the focused laser beam, and the MPD spectra became different as compared to those in Fig. 5 where they were obtained with the uniform laser beam.

4 Conclusion

The main conclusion of this work is that in the process of IR multiphoton excitation of the SiF₂H₂ molecules with the pulsed CO₂-laser radiation only a small part of the molecules interacts with the radiation due to the rotational bottleneck effect. This part was estimated as about 10%. Therefore, only less than 1% of the molecules can be excited up to the dissociation energy at appropriate radiation fluences (< 2 J/cm²).

The IR MPD spectrum of the difluorosilane molecule is quite narrow compared to the isotopic shift; so, the possibility of isotope-selective MPD exists.

This result, obtained for difluorosilane, could be generalized for almost all the molecules with as small a number of atoms as difluorosilane. Exceptions could be only the molecules with the same feature as CF₃I that 'fortunately' has several strong anharmonic resonances coupling almost all vibrational modes even at very low vibrational energy.

In other cases, to avoid the rotational bottleneck, one has to choose the molecule with essentially a large number of atoms as the object for isotope-selective multiphoton dissociation.

ACKNOWLEDGEMENTS This work was supported by the Russian Foundation for Basic Research (Grant No. 01-03-40101) and the Siberian Branch of the Russian Academy of Science (Grant No. 86-2000).

REFERENCES

- W.S. Capinski, H.J. Maris, E. Bauser, E. Silier, M. Asen-Palmer, T. Ruf, M. Cardona, E. Gmelin: *Appl. Phys. Lett.* **71**, 2109 (1997)
- K. Takyu, K.M. Itoh, K. Oka, N. Saito, V.I. Ozhogin: *Jpn. J. Appl. Phys.* **38**, 1493 (1999)
- J.L. Lyman, S.D. Rockwood: *J. Appl. Phys.* **47**, 595 (1976)
- N.K. Serdyuk, E.N. Chesnokov, V.N. Panfilov: *React. Kinet. Catal. Lett.* **17**, 19 (1981)
- M. Kamioka, S. Arai, Y. Ishikawa, S. Isomura, N. Takamiya: *Chem. Phys. Lett.* **119**, 357 (1985)
- M. Kamioka, Y. Ishikawa, H. Kaetsu, S. Isomura, S. Arai: *J. Phys. Chem.* **90**, 5727 (1986)
- H. Suzuki, H. Araki, T. Noda: *J. Jpn. Instrum. Methods* **61**, 145 (1997)
- J.L. Lyman, B.E. Newman, T. Noda, H. Suzuki: *J. Phys. Chem. A* **103**, 4227 (1999)
- M. Kamioka, Y. Ishikawa, S. Arai, S. Isomura, N. Takamiya: *Laser Sci. Prog. Rep. IPCR.* **7**, 57 (1985)
- CRC Handbook of Chemistry and Physics*, 79th edn., ed. by D.R. Lide (CRC, Boca Raton, Florida 1998) pp. 11-43
- S. Cradock, E.A.V. Ebsworth, A.G. Robiette: *Trans. Faraday Soc.* **60**, 1502 (1964)
- V.S. Letokhov, A.A. Makarov: *JETP* **63**, 2064 (1972) (in Russian)
- V. Tosa, S. Isomura, K. Takeuchi: *J. Photochem. Photobiol. A* **91**, 173 (1995)
- V.N. Bagratashvili, V.S. Doljikov, V.S. Letokhov, A.A. Makarov, E.A. Ryabov, V.V. Tyakht: *Sov. Phys. JETP* **50**, 1075 (1979)
- M. Quack: *Infrared Phys.* **29**, 441 (1989)
- M. Quack: *J. Mol. Struct.* **292**, 171 (1993)
- V.N. Bagratashvili, Y.G. Vainer, V.S. Doljikov, S.F. Kol'yakov, V.S. Letokhov, A.A. Makarov, L.P. Malyavkin, E.A. Ryabov, E.G. Sil'kis, V.D. Titov: *Sov. Phys. JETP* **53**, 512 (1981)
- W. Fuss: *Spectrochim. Acta* **38A**, 829 (1982)
- H.B. Schlegel: *J. Phys. Chem.* **88**, 6254 (1984)
- P. Ho, C.F. Melius: *J. Phys. Chem.* **94**, 5120 (1990)
- M. Koshi, S. Kato, H. Matsui: *J. Phys. Chem.* **95**, 1223 (1991)
- M.Y. Skok, E.N. Chesnokov: *Khim. Fiz.* **7**, 228 (1988) (in Russian)
- A.C. Station, A. Freedman, J. Wormhoudt, P.P. Gasper: *Chem. Phys. Lett.* **122**, 190 (1985)
- A. Freedman, K.E. McCurdy, J. Wormhoudt, P.P. Gasper: *Chem. Phys. Lett.* **142**, 255 (1987)
- K. Sugawara, F. Ito, T. Nakanaga, H. Takeo: *Chem. Phys. Lett.* **232**, 561 (1995)
- V.N. Bagratashvili, Y.G. Vainer, V.D. Dolgikov, V.S. Letokhov, A.A. Makarov, L.P. Maliavkin, E.A. Ryabov, A.C. Sil'kis: *Opt. Lett.* **6**, 148 (1981)
- A.L. Malinovsky, E.A. Ryabov, V.S. Letokhov: *Chem. Phys.* **139**, 229 (1989)
- P.J. Robinson, K.A. Holbrook: *Unimolecular Reactions* (Wiley-Interscience, London 1972)
- L.D. Landau, E.M. Lifshits: *Statistical Physics, Part 1* (Nauka, Moscow 1976) (in Russian)
- E.S. Medvedev: *Chem. Phys.* **41**, 103 (1979)
- W. Fuss: *Chem. Phys.* **36**, 135 (1979)
- M. Quack: *J. Chem. Phys.* **69**, 1282 (1978)
- J.L. Lyman: *J. Chem. Phys.* **67**, 1868 (1977)
- E.R. Grant, P.A. Shultz, A.S. Sudbo, Y.R. Shen, Y.T. Lee: *Phys. Rev. Lett.* **40**, 115 (1978)
- J.C. Stephenson, D.S. King, M.F. Goodman, J. Stone: *J. Chem. Phys.* **70**, 4496 (1979)
- V.S. Letokhov: *Nonlinear Laser Chemistry: Multiple-Photon Excitation* (Springer, Berlin 1983)
- A.J. Colussi, S.W. Benson, R.J. Hwang, J.J. Tice: *Chem. Phys. Lett.* **52**, 349 (1977)
- R.D. Levine, A. Ben-Shaul: in *Chemical and Biochemical Application of Lasers, Vol. II*, ed. by C.B. Moore (Academic, New York 1977)
- C.C. Jensen, J.I. Steinfeld, R.D. Levine: *J. Chem. Phys.* **69**, 1432 (1978)
- M.W. Schmidt, K.K. Baldrige, J.A. Boatz, S.T. Elbert, M.S. Gordon, J.H. Jensen, S. Koseki, N. Matsunaga, K.A. Nguyen, S. Su, T.L. Windus, M. Dupuis, J.A. Montgomery: *J. Comput. Chem.* **14**, 1347 (1993)